IEEE Access
Multidisciplinary | Rapid Review | Open Access Journal

Received December 11, 2020, accepted December 25, 2020, date of publication January 5, 2021, date of current version January 13, 2021.

Digital Object Identifier 10.1109/ACCESS.2021.3049293

Active Thermal Control for Modular Power Converters in Multi-Phase Permanent Magnet Synchronous Motor Drive System

HAO YAN[1], (Member, IEEE), WEIDUO ZHAO[2], (Member, IEEE), GIAMPAOLO BUTICCHI[2], (Senior Member, IEEE), AND CHRIS GERADA[3], (Senior Member, IEEE)

[1]School of Civil Aviation, Northwestern Polytechnical University, Xi'an 710072, China
[2]Key Laboratory of More Electric Aircraft Technology of Zhejiang Province, University of Nottingham Ningbo China, Ningbo 315100, China
[3]Power Electronics, Machines and Control Group, University of Nottingham, Nottingham NG7 2RD, U.K.

Corresponding author: Weiduo Zhao (zhaoweiduo@gmail.com)

This work was supported in part by the National Natural Science Foundation of China under Grant 51807099 and Grant 51807100.

ABSTRACT Modular winding structure has been employed in the Permanent Magnet Synchronous Motors (PMSMs) to increase the reliability and reduce the torque ripple. Nevertheless, the reliability of the motor system depends on the lifetime of the power semiconductor devices. Since the thermal cycles, which can generate the mechanical stress between the different material layers in power devices, are the key factors to influence the lifetime of power devices, in this paper, an Active Thermal Control (ATC) for modular power converters in PMSM drive is proposed to extend the system lifetime. The power routing method is employed to balance the power in a quadruple modular winding PMSM system. The Rainflow Counting Algorithm is used to calculate the thermal cycles with a load mission profile, and estimate the lifetime of the power converters. The proposed method is validated by both simulation and experiments.

INDEX TERMS Active thermal control, multi-phase motor, permanent magnet synchronous motor, modular inverter, motor control.

I. INTRODUCTION

In recent years, the thermal control of power converters has been widely used in power electronics applications to improve system reliability [1], [2]. As for the motor drive application, especially the multi-phase motor, the thermal control for motor drive can also be adopted. For instance, the multi-phase Permanent Magnet Synchronous Motor (PMSM), it is widely used in servo applications in high reliability demand, for instance aerospace, electric vehicle and undersea equipment [3], [4]. Multi-unit, modular winding as well as redundant structure are effective ways to increase the reliability of multi-phase PMSM [5]. At the same time, with the power electronics application increasing rapidly, multi-level and multi-phase converters are applied in the control system of multi-phase PMSM, which is beneficial to the motor drive performance and its reliability [6].

The associate editor coordinating the review of this manuscript and approving it for publication was Zhuang Xu.

In [5], an approach about driving a five-phase induction motor with a five-leg voltage source inverter. This paper gives an analysis on the drive performance of the multi-phase modular winding machine, and it is pointed out that the structure can effectively reduce the influence of space harmonic on the motor. In order to add the capacity of conventional three-phase machine control system, different kinds of multi-level converters are discussed in [7]. The five-level inverter can be used in high voltage drive and the output voltage Total Harmonic Distortion (THD) is reduced. In [8], the multi-level converter is used to drive a three-phase motor with sensorless control. In [9], a method of driving the open-winding PMSM is studied, the six-phase machine it driven by two three-level voltage source inverters, which is an effective way to reduce the torque ripples. Besides, the model predictive direct flux vector control with model predictive based method is applied to the control of an induction motor with multi-unit winding structure [10].

In power converter, the reliability of semiconductor devices is the key reason to determine the lifetime. Therefore, it is

very important to make sure the power switches are in high reliability state. One of the main causes of failure of electrical equipment and capacitors is thermo-mechanical fatigue at different material connections [11]. Fig. 1 shows the basic structure of a power device with different materials stacked on a direct-band-copper (DBC) substrate. Since the thermal expansion coefficients (CTE) of copper and ceramic of the substrate are different, the temperature variations, also called thermal cycles, can generate the mechanical stress between the material layers [12]. The thermal cycle then causes the material to expand and contract, leading to aging. It is well known that thermal cycle magnitude is a key parameter affecting the life of power semiconductor devices [13].

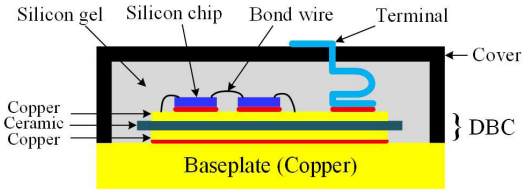

FIGURE 1. Basic structure of a power semiconductor device [12].

In recent years, Active Thermal Control (ATC) in power electronics system has become an effective method to reduce the thermal cycling of power switch [14]. ATC is usually achieved by lowering the amplitude of fluctuation or the average temperature without modifying the design of the power converter [11], [15], [16]. Several kinds of ATC methods had been presented in [13], [17], [18] with the aim of reducing thermal stress in power modules.

However, most ATC algorithms focus on reducing the thermal cycle of a power converter or even a power device.Power routing is a method of transferring power between modules of modular power converters to reduce the thermal stress of the modules and thus reduce the residual life of the modules [19]. Its application in modular drive of multi-phase motor has not been reported in literature. Considering the high reliability requirement of modular winding PMSM application, the performance of motor system can be further improved by improving the reliability of power converter and prolonging its lifetime. For example, the lifetime of the whole motor system is determined by the lifetime of the weaker modular converter due to the constant maintenance of the motor drive system and the different lifetime of the power converter. However, ATC based on power routing can balance the liftimee of different power converters, thus further improving the reliability of the system.

In order to solve the above problems, this paper presents an ATC method for the power converter of a quadruple modular winding PMSM. Based on the measured temperature, the Rainflow Couting Algorithm is used to estimate the cumulative damage of the converter. The power routing method can effectively control the life of the system and reduce the power of the system in the case of large cumulative damage. ATC aims to extend the lifetime of the weaker power converter, and the routing of the total power depends on the estimated lifetime.

An initial version of the manuscript was presented at the IEEE CPE-POWERENG 2019 [20], with respect to the initial submission, this paper presents a deeper reliability study and an experimental verification of a multi-phase winding drive. The paper is organized as follows. Section II describes the lifetime estimation method of power converters. In Section III, the system and the proposed ATC method for modular power converters are introduced. A simulation model is established and the simulation results are prosented in Section IV. The experimental validation is made in Section V before the conclusions are presented in Section VI.

II. LIFETIME ESTIMATION OF POWER CONVERTERS

A. BASIC PRINCIPLES OF LIFETIME ESTIMATION

In power converters, the failure of components such as capacitors and power semiconductors will affect their lifetime. Only faults in power semiconductor are considered in this paper. In actual situation, the power semiconductor manufacturers usually provide the time to failure by the number of thermal cycles to failure N_f. According to this, a well-known method, called Coffin-Manson-Arrhenius model [21], to estimate the lifetime of power semiconductors is expressed as following equation.

$$N_f = k_1 \cdot \Delta T^{-k_2} \cdot e^{\frac{k_3}{k_B T_{j,av}}} \tag{1}$$

where ΔT is the magnitude of the thermal cycles, $T_{j,av}$ is the average junction temperature during the thermal cycle. k_1, k_2, k_3 are the fitting parameters extracted from multiple reliability experiments. k_B is the Boltzmann constant.

In practice, the mission profile of the power converter is uncertain, so a direct derivation of the accumulated damage with (1) is not suitable for estimate the lifetime. Therefore, the cycle counting method is needed to decompose the temperature curve. In this case, rain Rainflow Counting Algorithm is widely used in cyclic fatigue analysis [22]. Then, the Miner's rule, expressed as (2), can be adopted to obtain the accumulated damage [23].

$$D_a = \sum_i \frac{n_i}{N_i} \tag{2}$$

Here, D_a is the accumulated damage, n_i the number of cycles in the stress range i, and N_i the number of cycles to failure in the i_{th} stress range. Therefore, with the increase of the number of thermal cycles in the mission profile, the cumulative damage of the power devices will increase. Once the value of D_a reaches 1, the power device will be in failure [11]. The reciprocal of cumulative damage is used to describe the number of thermal cycles that the module can withstand, so that the lifetime of the module can be calculated.

B. RAINFLOW COUNTING ALGORITHM

The lifetime of power semiconductor devices depends on a variable mission profile, and Rainflow Counting Algorithm

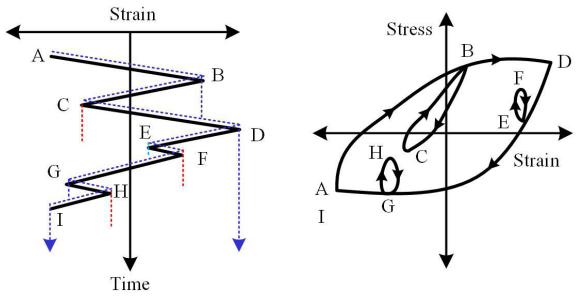

FIGURE 2. Load sequence and stress-strain cycles in Rainflow Counting Algorithm.

is an effective method to reduce the complex mission profile to some key events that can be used for life estimation. Fig. 2 illustrates the principles of Rainflow Counting Algorithm. When this method is applied to power converters, thermal expansion, stress and strain should be considered. In this application, the strain is based on the ratio of the change in the length of the material to the actual length based on the temperature change [24].

Typically, Rainflow Counting Algorithm is used to extract cycles from load history, which can be obtained from temperature measurement. According to the temperature-time curve, the extreme value and minimum value of the temperature-time curve are obtained, and the full cycles and half cycles are defined accordingly. Finally, the lifetime is estimated using these cycles.

III. PROPOSED ACTIVE THERMAL CONTROL FOR QUADRUPLE MODULAR WINDING PMSM DRIVE

In this section, the proposed ATC method based on power routing in modular PMSM drive is presented, and the realization of the algorithm is explained.

A. SYSTEM DESCRIPTION OF MOTOR DRIVE SYSTEM

The proposed ATC method is introduced by taking the quadruple modular PMSM drive system as an example. The motor drive system is shown in Fig. 3.

Each power converter is a two-level pulse width modulation voltage source inverter (PWM-VSI), and the three power converters share the same dc-link voltage v_{dc}. Given this parallel structure, the power of each converter can be expressed as (3). Here, p_{con1}, p_{con2}, p_{con3} and p_{con4} are the power of each inverter, and i_{dc1}, i_{dc2}, i_{dc3} and i_{dc4} the dc-link current of each inverter.

$$\begin{cases} p_{con1} = v_{dc} \cdot i_{dc1} \\ p_{con2} = v_{dc} \cdot i_{dc2} \\ p_{con3} = v_{dc} \cdot i_{dc3} \\ p_{con4} = v_{dc} \cdot i_{dc4} \end{cases} \tag{3}$$

More, the total power p_{dc} equals to

$$p_{dc} = p_{con1} + p_{con2} + p_{con3} + p_{con4} \tag{4}$$

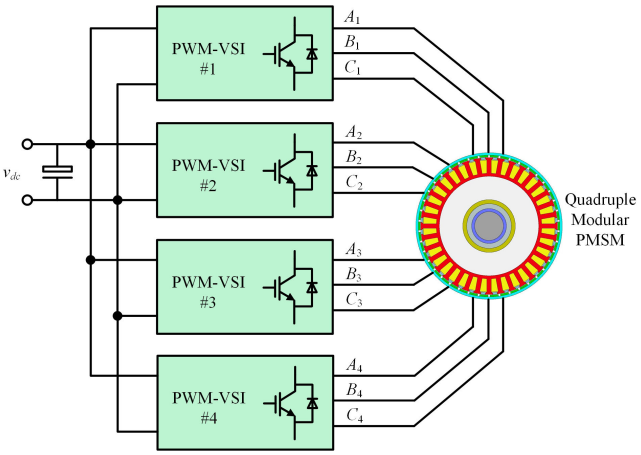

FIGURE 3. Quadruple modular winding PMSM drive system.

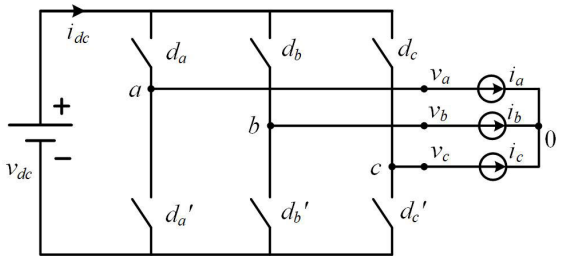

FIGURE 4. Equivalent circuit of PWM-VSI.

Fig. 4 shows the equivalent circuit of one PWM-VSI. In this figure, $d_a \sim d_c$, $d_a' \sim d_c'$ are the duty cycles of the related power switch, v_a, v_b and v_c are the three-phase terminal voltage, and i_a, i_b and i_c are the three-phase current.

The dc-link current can be calculated as

$$i_{dc} = i_a d_a + i_b d_b + i_c d_c \tag{5}$$

Assuming that the power converter losses are neglected, let $p_{dc} = p_{ac}$. By using the PARK coordinate transformation, the power of one PWM-VSI can be expressed as

$$p_{dc} = v_{dc} \cdot i_{dc} = \frac{3}{2}\left(v_d i_d + v_q i_q\right) = p_{ac} \tag{6}$$

Here, v_d, v_q, i_d and i_q are the voltage and current components under $d-q$ rotary coordinate system.

Combining (3), the power of the four power converters can be calculated as

$$\begin{cases} p_{con1} = v_{dc} \cdot i_{dc1} = \frac{3}{2}\left(v_{d1} i_{d1} + v_{q1} i_{q1}\right) \\ p_{con2} = v_{dc} \cdot i_{dc2} = \frac{3}{2}\left(v_{d2} i_{d2} + v_{q2} i_{q2}\right) \\ p_{con3} = v_{dc} \cdot i_{dc3} = \frac{3}{2}\left(v_{d3} i_{d3} + v_{q3} i_{q3}\right) \\ p_{con4} = v_{dc} \cdot i_{dc4} = \frac{3}{2}\left(v_{d4} i_{d4} + v_{q4} i_{q4}\right) \end{cases} \tag{7}$$

In this paper, the tested motor is a surface-mounted PMSM, so the $i_d = 0$ method is used to obtain the maximum torque.

Therefore, (7) can be simplified as (8). It can be seen that the values of q-axis current in each winding will determine the power in each converter.

$$\begin{cases} p_{con1} = v_{dc} \cdot i_{dc1} = \dfrac{3}{2} v_{q1} i_{q1} \\ p_{con2} = v_{dc} \cdot i_{dc2} = \dfrac{3}{2} v_{q2} i_{q2} \\ p_{con3} = v_{dc} \cdot i_{dc3} = \dfrac{3}{2} v_{q3} i_{q3} \\ p_{con4} = v_{dc} \cdot i_{dc4} = \dfrac{3}{2} v_{q4} i_{q4} \end{cases} \tag{8}$$

Normally, the load of power converter should be in a random situation, and a function of time. For instance, in Fig. 5, the read line indicates the variation of the motor load, which is called load mission profile. In the Y-axis, 100% means full load, and all the four power converters should provide the maximum power in this situation. If the Y value is under 100%, it means some power converters are not in rated power. The power determines the current, so the load mission profile is the key factor of converter temperate as well as the lifetime. Therefore, this profile is used to validate the proposed ATC method.

B. THERMAL-BASED POWER ROUTING ALGORITHM

In some conditions, the temperature of one certain converter is the highest and its thermal cycles is larger than the other, then the motor system lifetime is determined by this weakest converter. One way to reduce its temperature is to transfer some power to other converters, which can reduce the thermal stress. This way is called power routing, and by doing this, the weakest converter lifetime is increasing, so is the whole motor drive system [2].

Power routing is a method of balancing the uneven load units in modular converters and then controlling the thermal stress of all power components in one module, which has been used in smart transformers [25], [26]. This method can equalize the useful remaining lifetime of the modular power converter [27].

Define m_{d1}, m_{d2}, m_{d3} and m_4 are the power distribution coefficients of the four converters, and calculated as

$$\begin{cases} m_{d1} = \dfrac{p_{con1}}{p_{dc}} \\ m_{d2} = \dfrac{p_{con2}}{p_{dc}} \\ m_{d3} = \dfrac{p_{con3}}{p_{dc}} \\ m_{d4} = \dfrac{p_{con4}}{p_{dc}} \end{cases} \tag{9}$$

More, in (9), $m_{d1} + m_{d2} + m_{d3} + m_{d4} = 1$. In a normal operation, the power distribution coefficients are equally distributed as

$$m_{d1} = m_{d2} = m_{d3} = m_{d4} = \frac{1}{4} \tag{10}$$

However, in ATC algorithms, the temperature of power modules decides the power distribution coefficients.

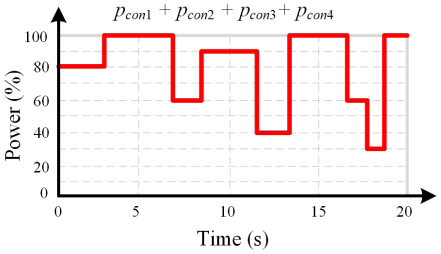

FIGURE 5. Load mission profile.

In Fig. 6, the block diagram of the proposed ATC algorithm for quadruple modular winding PMSM drive is presented.

According to (8), the power in each converter can be routed with the control of q-axis current loop. The load mission profile determine the total power reference p^*_{dc}, which is ranged from 0 to 1. Thermocouples are placed on each power module and get the junction temperature. The temperature references are given by software and compared with the measured temperature, then the thermal controller calculates the four power distribution coefficients m^*_{d1}, m^*_{d2}, m^*_{d3} and m^*_{d4}, which are used to obtain the power references of the four converters p^*_{con1}, p^*_{con2}, p^*_{con3} and p^*_{con4}. Based on the FOC control for PMSM, the d-axis and q-axis current references of four current loops are obtained and then the Space Vector PWM signals are generated to operate the PMSM.

The basic principles of ATC are explained in Fig. 6. To clearly illustrate the implementation of the quadruple modular winding PMSM FOC drive, the block diagram of the speed and current double-close-loop motor control algorithm is shown in Fig. 7. In the speed controller, the motor speed reference and measured motor speed are compared and calculated with a Proportional-Integral (PI) controller. The d-axis and q-axis current references are calculated with ATC algorithm. Since the motor is a surface-mounted PMSM, the four d-axis current references i^*_{d1}, i^*_{d2}, i^*_{d3} and i^*_{d4} should be set as zero. Eight PI controllers are used to control the current loop and four reference voltage vectors are obtained as the output of the current loop. Then, based on Space Vector PWM calculation, the PWM signals to drive the power converters are obtained. Finally, the modular winding PMSM is driven by the four PWM-VSIs.

IV. SIMULATION VALIDATION

A. SIMULATION MODEL BUILD

Simulation model is built with software PLECS to validate the proposed method. The quadruple modular winding PMSM is with a 48-slot-8-pole structure, and the motor drive parameters are presented in Table 1.

Thermal circuit model is established to calculate and analyze the temperature of each power converter. Taken one power converter as example, its thermal model is illustrated in Fig. 8, and there are four hear sinks attached on the power module, with the same thermal chains.

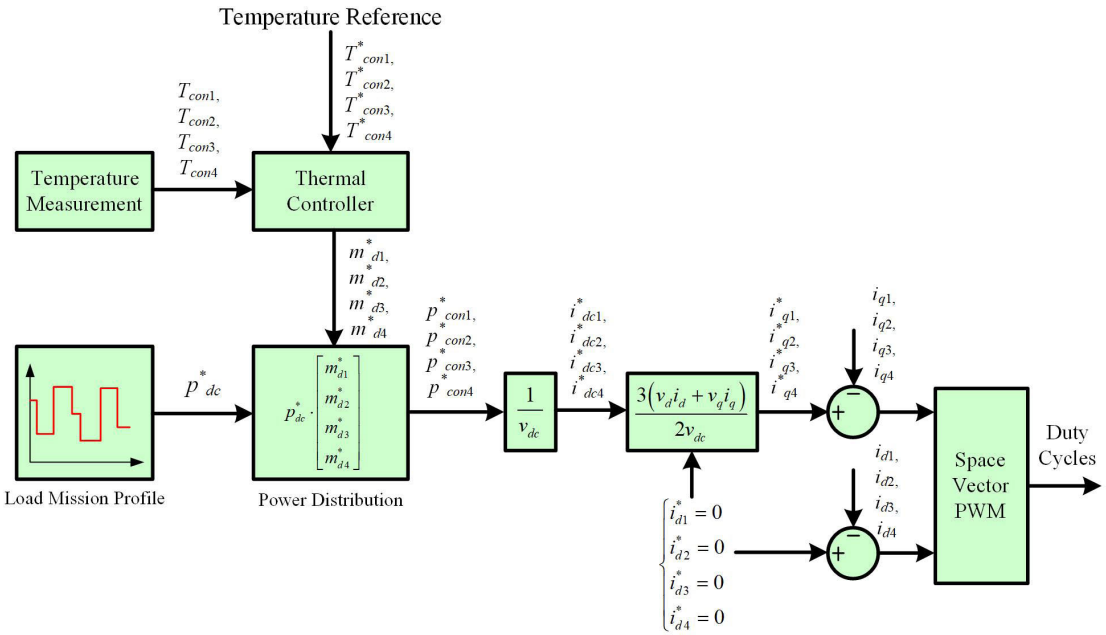

FIGURE 6. Block diagram of the proposed ATC.

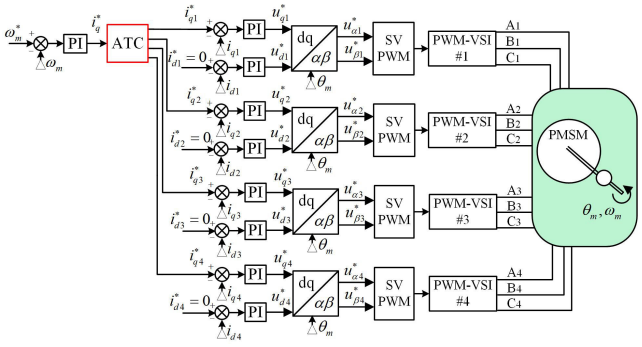

FIGURE 7. Block diagram of the speed and current double-close-loop control for the quadruple modular winding PMSM.

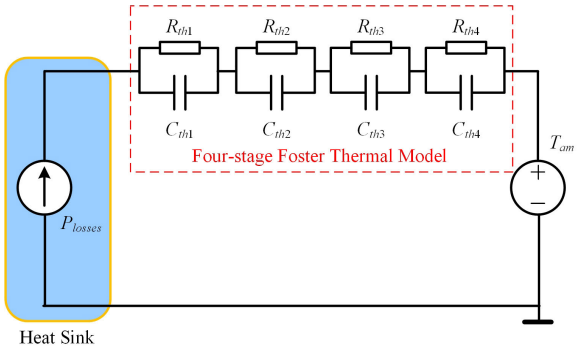

FIGURE 8. Thermal model of the power converter.

TABLE 1. Parameters of PMSM Drive System.

Parameters	Quantity
Winding resistance (R_a)	0.018 Ω
Winding inductance (L_a)	0.624 mH
Flux linkage (φ_m)	0.067 Vs
Moment of inertia (J)	0.00082 N·ms^2
Number of pole pairs (p)	4
DC-link voltage (V_{dc})	100 V
Rated torque (T_N)	8 N·m
Rated speed (n_N)	500 r/min
PWM frequency (f_{pwm})	10 kHz

The thermal simulation model in built in PLECS environment, and the ambient temperature T_{am} is set as 50℃, which can speed up the simulation process. According to [28], a four-stage Foster thermal model is used as the thermal chain. There are four thermal resistors and four thermal capacitors in the thermal chain, and the thermal parameters are set as follows: $R_{th1} = 0.0903$ K/W, $R_{th2} = 0.361$ K/W, $R_{th3} = 0.203$ K/W, $R_{th4} = 0.141$ K/W, $C_{th1} = 0.0023$ J/K, $C_{th2} = 0.0282$ J/K, $C_{th3} = 0.113$ J/K, $C_{th4} = 0.282$ J/K. In the PLECS simulation, the thermal model of the IGBT and diodes are build according to the values in datasheet of the power module (FS50R06W1E3), and the details of the thermal models have been added in the appendix. The lookup tables should be written in the component thermal model. After the thermal model is established, the switching losses and conduction losses of IGBTs and diodes are calculated with PLECS, and the junction temperature of power devices and the temperature of heatsinks are obtained.

To validate the proposed method, the thermal resistance and thermal capacitance of PWM-VSI#1 is tuned high, which can simulate the temperature differences between the other three converters. As for the actual working condition, due to the different heat dissipation conditions, the temperature of each power module is not uniform.

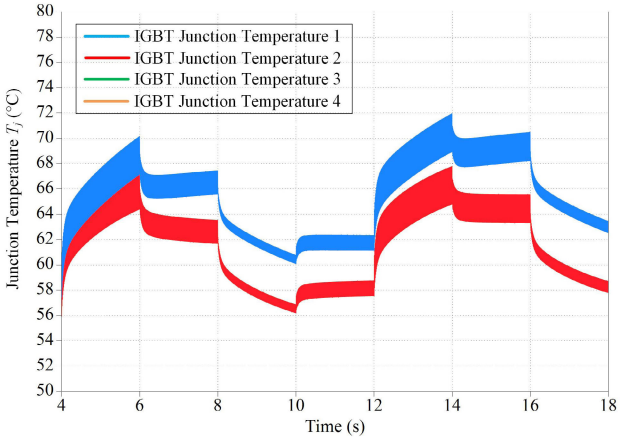

FIGURE 9. Simulation results of IGBT junction temperature in each power converter. (a) Without ATC. (b) With ATC.

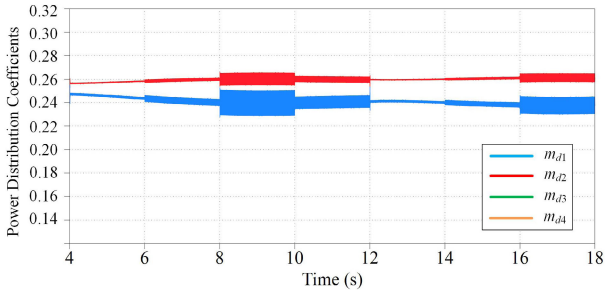

FIGURE 10. Power distribution coefficients of each converter under ATC.

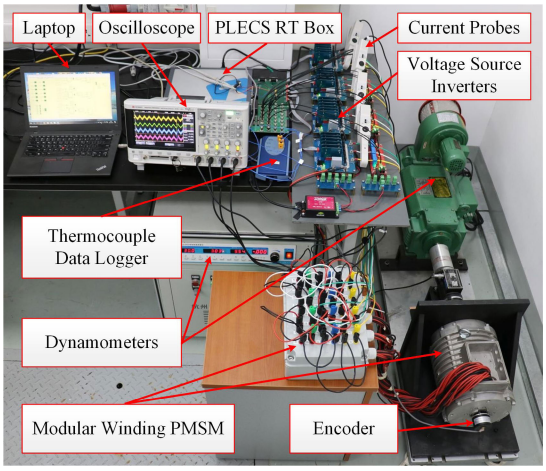

FIGURE 11. The photo of the experimental validation platform.

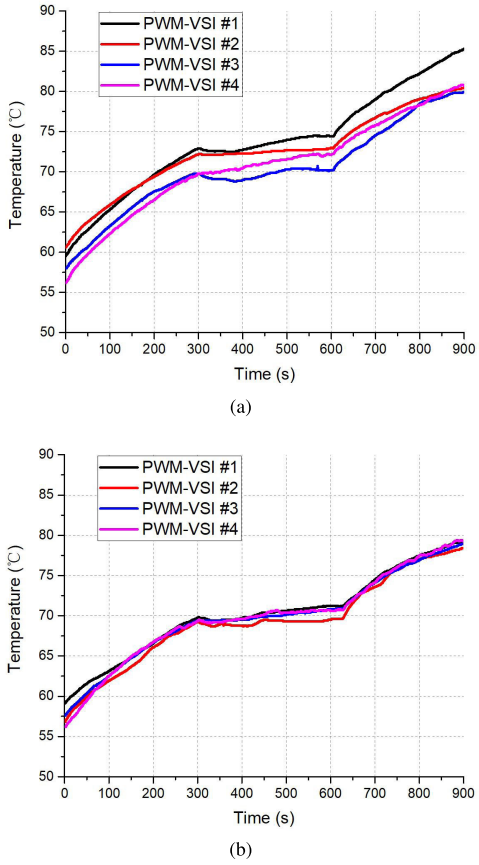

FIGURE 12. Case temperature of the power switches in four PWM-VSIs. (a) Without ATC. (b) With ATC.

B. SIMULATION RESULTS

The junction temperature of the power switches in four power converters with and without the proposed ATC is presented in Fig. 9. To simulate the temperature fluctuations, the load mission profile is set as the power reference, which changes every two seconds. To make the temperature of the four power converters different, the values of the thermal chain of PWM-VSI#1 is set larger than the other three. Besides, maintain the thermal chain parameters of the other three power modules as the same, and then the simulation waveforms of PWM-VSI#2, PWM-VSI#3 and PWM-VSI#4 are overlapped. From the simulation results, it can be seen that the junction temperature T_j in the PWM-VSI#1 is reduced when ATC employed. For instance, at the instant $t = 14$ s, T_j of PWM-VSI#1 decreases from 70.93℃ to 69.19℃ with ATC.

Fig. 10 shows the power distribution coefficients of the four converters with ATC. The blue waveform is the power

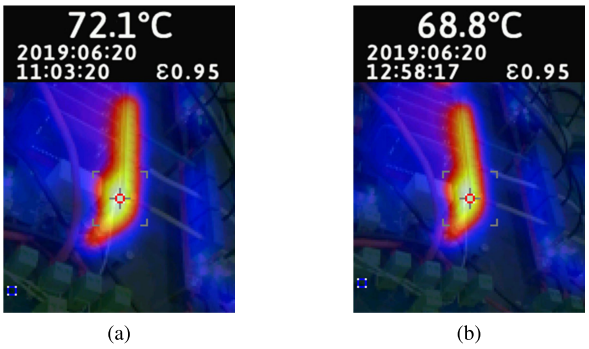

FIGURE 13. Temperature distribution of the PWM-VSI#1. (a) Without ATC. (b) With ATC.

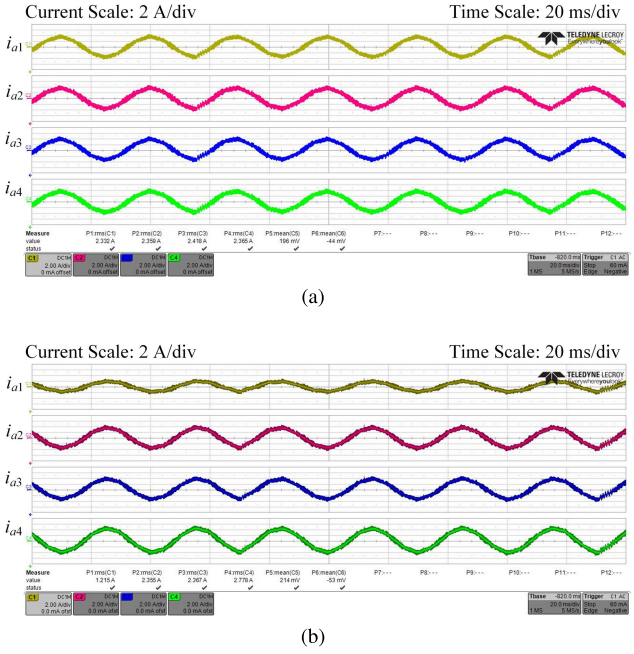

FIGURE 14. Experimental results of phase current waveform of the PMSM. (a) Without ATC. (b) With ATC.

distribution coefficient m_{d4}, and the value is lower than the other three coefficients due to the high junction temperature in PWM-VSI#1.

V. EXPERIMENTAL VALIDATION

To further validate the porposed method, a quadruple modular PMSM with a 48-slot/8-pole structure is used to build the motor drive platform. Table 1 gives the motor parameters. The photo of the experimental validation platform is shown in Fig. 11. The control unit is the PLECS RT Box, which generates 24 channels of PWM signals and then drive four PWM-VSIs. The four inverters share the same DC power supply. Behind the PWM-VSIs, there are four current sensor boards to sample the phase current, and the hall-effect current sensors is with 50 kHz sampling rate, which is LEM HAIS-50P. The current sensor boards transfer the sampling results to the A/D ports of the control unit. In each PWM-VSI, the power switches are driven by the PWM signals with 10 kHz switching frequency. Moreover, to obtain the

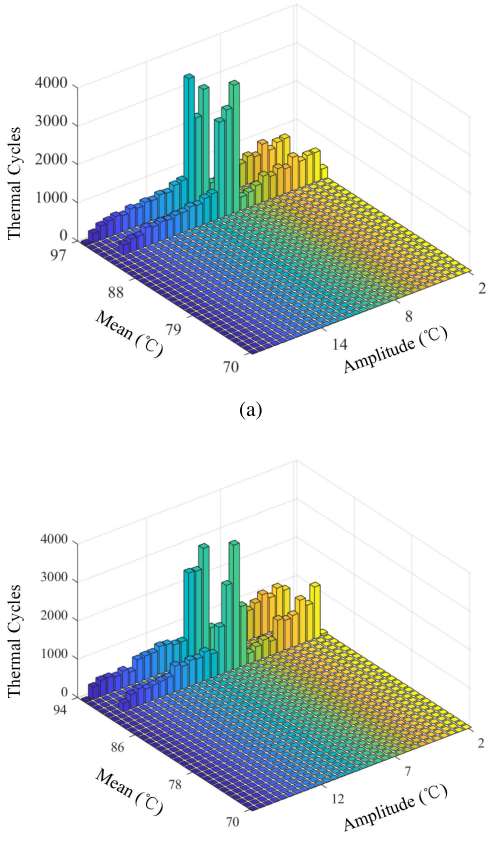

FIGURE 15. Number of thermal cycles calculated by Rainflow Counting Algorithm. (a) Without ATC. (b) With ATC.

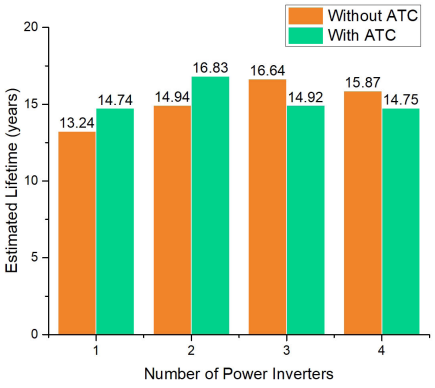

FIGURE 16. Estimated lifetime of the power switches in four PWM-VSIs before and after the proposed ATC.

temperature of the PWM-VSIs, a thermocouple data logger is put near the inverters, and the sampling frequency of the temperature data is 10 Hz.

Fig. 12 shows the temperature of four inverters, and the thermocouple probes are placed between one power switch and its heatsink. The time scale of the load mission profile is 900 seconds, and the load of the motor is changed by the upper control monitor every 300 seconds. The results, in the figure, indicate that the proposed ATC is an effective

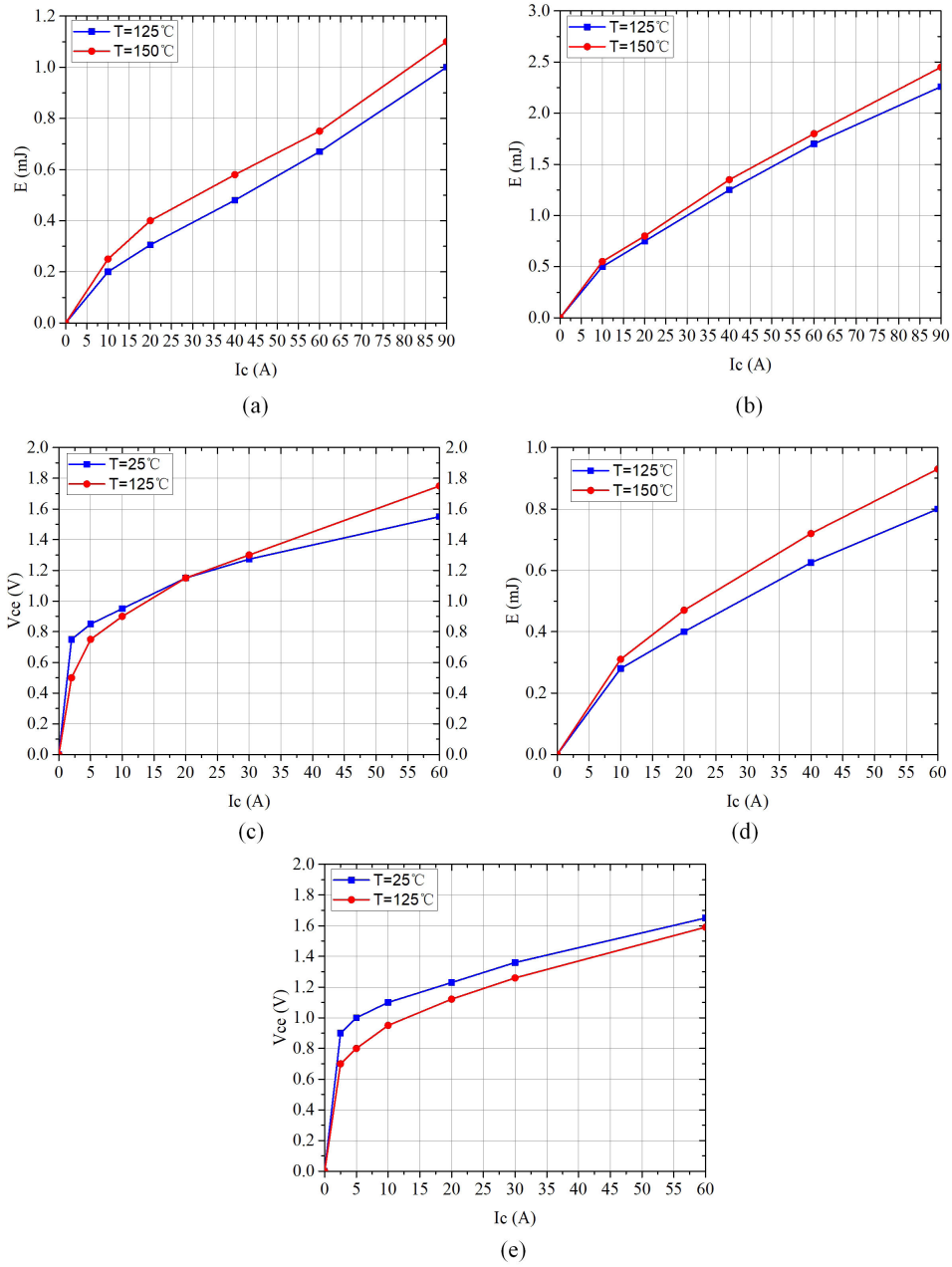

FIGURE 17. Loss model in PLECS simulation; (a) IGBT turn-on, (b) IGBT turn-off, (c) IGBT conduction, (d) Diode turn-off, and (e) Diode conduction.

approach to balance the temperature of the PWM-VSIs. Without the ATC, the power switch in PWM-VSI#1 is the highest, however, the temperature of PWM-VSI#1 is reduced obviously and the power routing between the inverters keeps the four temperature data the same. For example, the maximum case temperature of PWM-VSI#1 is reduced from 85.3℃to 79.3℃. The changing of the temperature curve is caused by the load mission profile in the experiments, and one experiment lasts fifteen minutes. Furthermore, an infrared camera is used to capture the temperature distribution of PWM-VSI#1. As illustrated in Fig. 13 (a) and (b), the maximum temperature without ATC and with ATC is 72.1℃ and 68.8℃, respectively. The IR camera pictures are taken at the same instant during the two experiments, which share the same load mission profile. Therefore, the proposed ATC with power routing method is effective to control the temperature of power switches in the quadruple modular winding PMSM drive system.

Fig. 14 (a) and (b) present the experimental data of Phase A current of the four modular windings i_{a1}, i_{a2}, i_{a3} and i_{a4} without and with the proposed ATC method, respectively. A comparison of the two results reveals that the phase current

of PWM-VSI#1 decreases when ATC is employed. Since the temperature of PWM-VSI#1 is the highest among the four inverters, the current and power of PWM-VSI#1 should be routed to the other inverters for reducing its temperature, which is beneficial to its lifetime.

To further verify the effectiveness of the proposed ATC on the inverter lifetime, the temperature data is processed with Rainflow Counting Algorithm. The case temperature of the power switches is obtained from the thermocouple data logger, and the junction temperature of power switches is estimated by the Foster thermal model. The number of thermal cycles, mean value and amplitude value of the junction temperature can be calculated by Rainflow Counting Algorithm. The load mission profile is repeated for eight hours per day. Fig. 15 illustrates the thermal cycles before and after the ATC. It is obvious that the number of thermal cycles is decreased with ATC, which means that the proposed method can reduce the thermal stress in power switches.

Fig. 16 shows the estimated lifetime before and after the ATC. Since the temperature of PWM-VSI#1 is the highest, its lifetime without ATC is the shortest, which is only 13.24 years. With the ATC, its lifetime is increased to 14.74 years. It can be concluded form the estimated lifetime that lifetime of the whole drive system is increased and the reliability is improved.

Taken together, these results suggest that the proposed ATC based on power routing method can balance the temperature of the power converters in the quadruple modular winding PMSM drive system. Although the power of each unit motor are different, the temperature of the PWM-VSIs are almost identical, which can increase the lifetime of the weakest inverter and then improve the reliability of the motor system.

VI. CONCLUSION

To enhance the reliability in the quadruple modular winding PMSM drive system, an ATC method based on power routing is proposed. Based on the theoretical analysis and the simulation and experimental results, some points can be concluded.

1) In the simulation results, the junction temperature of the power switches reduces with ATC. More, the power distribution coefficient of the weaker inverter is decreased, which can reduce the thermal cycles. And in the experiments, results suggest that the proposed ATC based on power routing method can balance the temperature of the four PWM-VSIs. The maximum case temperature of PWM-VSI#1 is reduced from 85.3℃to 79.3℃.

2) In the experiments, the junction temperature of the power switches can not be measured directly, so a four-stage Foster thermal network is used to estimate the junction temperature based on the case temperature data which is obtained by the thermocouple probes. By using the Rainflow Counting Algorithm, the lifetime of the power switches is estimated with the junction temperature data. From the results, the lifetime of the weakest inverter is increased from 13.24 years to 14.74 years.

3) Since the power among the four PWM-VSIs are different, the phase current of each modular winding are different. From the experiments, the motor drive performance before and after the ATC are almost the same, which verifies that the normal operation of the PMSM is not affected by the proposed method.

In all, the proposed method is an effective approach to increase the lifetime and reliability of the power converters in the quadruple modular winding PMSM drive system.

APPENDIX

In the PLECS simulation, the thermal model of the IGBT and diodes are build according to the values in datasheet of the power module (FS50R06W1E3). The details of the thermal models have been added in an appendix, as common practice in [29]. The loss model is shown in Fig. 17. For the IGBT model, the switching losses (turn-on and turn-off) and the conduction losses are considered, whereas the turn-on losses are ignored in the diode model since it is negligible.

REFERENCES

[1] V. G. Monopoli, A. Marquez, J. I. Leon, Y. Ko, G. Buticchi, and M. Liserre, "Improved harmonic performance of cascaded H-bridge converters with thermal control," *IEEE Trans. Ind. Electron.*, vol. 66, no. 7, pp. 4982–4991, Jul. 2019.

[2] A. Marquez, J. I. Leon, S. Vazquez, and L. G. Franquelo, "Closed-loop active thermal control via power routing of parallel DC-DC converters," in *Proc. IEEE 12th Int. Conf. Compat., Power Electron. Power Eng. (CPE-POWERENG)*, Apr. 2018, pp. 1–6.

[3] W. Zhang, Y. Xu, H. Huang, and J. Zou, "Vibration reduction for dual-branch three-phase permanent magnet synchronous motor with carrier phase-shift technique," *IEEE Trans. Power Electron.*, vol. 35, no. 1, pp. 607–618, Jan. 2020.

[4] Y. Huang, Y. Xu, W. Zhang, and J. Zou, "PWM frequency noise cancellation in two-segment three-phase motor using parallel interleaved inverters," *IEEE Trans. Power Electron.*, vol. 34, no. 3, pp. 2515–2525, Mar. 2019.

[5] A. S. Abdel-Khalik and S. Ahmed, "Performance evaluation of a five-phase modular winding induction machine," *IEEE Trans. Ind. Electron.*, vol. 59, no. 6, pp. 2654–2669, Jun. 2012.

[6] Z. Pan and R. A. Bkayrat, "Modular motor/converter system topology with redundancy for high-speed, high-power motor applications," *IEEE Trans. Power Electron.*, vol. 25, no. 2, pp. 408–416, Feb. 2010.

[7] H. Hosoda and S. Peak, "Multi-level converters for large capacity motor drive," in *Proc. Int. Power Electron. Conf. (ECCE ASIA)*, Jun. 2010, pp. 516–522.

[8] S. Kamel, S. Mark, and A. Greg, "Sensorless control of induction motors using multi-level converters," *IET Power Electron*, vol. 5, no. 2, pp. 269–279, Feb. 2012.

[9] K. K. Nallamekala and K. Sivakumar, "A fault-tolerant dual three-level inverter configuration for multipole induction motor drive with reduced torque ripple," *IEEE Trans. Ind. Electron.*, vol. 63, no. 3, pp. 1450–1457, Mar. 2016.

[10] S. Rubino, R. Bojoi, S. A. Odhano, and P. Zanchetta, "Model predictive direct flux vector control of Multi-three-Phase induction motor drives," *IEEE Trans. Ind. Appl.*, vol. 54, no. 5, pp. 4394–4404, Sep. 2018.

[11] M. Andresen, K. Ma, G. Buticchi, J. Falck, F. Blaabjerg, and M. Liserre, "Junction temperature control for more reliable power electronics," *IEEE Trans. Power Electron.*, vol. 33, no. 1, pp. 765–776, Jan. 2018.

[12] B. Ji, V. Pickert, W. Cao, and B. Zahawi, "*In situ* diagnostics and prognostics of wire bonding faults in IGBT modules for electric vehicle drives," *IEEE Trans. Power Electron.*, vol. 28, no. 12, pp. 5568–5577, Dec. 2013.

[13] M. Andresen, V. Raveendran, G. Buticchi, and M. Liserre, "Lifetime-based power routing in parallel converters for smart transformer application," *IEEE Trans. Ind. Electron.*, vol. 65, no. 2, pp. 1675–1684, Feb. 2018.

[14] P. Kumar Prasobhu, V. Raveendran, G. Buticchi, and M. Liserre, "Active thermal control of GaN-based DC/DC converter," *IEEE Trans. Ind. Appl.*, vol. 54, no. 4, pp. 3529–3540, Jul. 2018.
[15] V. Blasko, R. Lukaszewski, and R. Sladky, "On line thermal model and thermal management strategy of a three phase voltage source inverter," in *Proc. Conf. Rec. IEEE Ind. Appl. Conf. 34th IAS Annu. Meeting*, vol. 2, Oct. 1999, pp. 1423–1431.
[16] M. Weckert and J. Roth-Stielow, "Lifetime as a control variable in power electronic systems," in *Proc. Emobility-Electr. Power Train*, Nov. 2010, pp. 1–6.
[17] D. A. Murdock, J. E. R. Torres, J. J. Connors, and R. D. Lorenz, "Active thermal control of power electronic modules," *IEEE Trans. Ind. Appl.*, vol. 42, no. 2, pp. 552–558, Mar. 2006.
[18] M. Andresen, G. Buticchi, and M. Liserre, "Study of reliability-efficiency tradeoff of active thermal control for power electronic systems," *Microelectron. Rel.*, vol. 58, pp. 119–125, Mar. 2016.
[19] M. Liserre, M. Andresen, L. Costa, and G. Buticchi, "Power routing in modular smart transformers: Active thermal control through uneven loading of cells," *IEEE Ind. Electron. Mag.*, vol. 10, no. 3, pp. 43–53, Sep. 2016.
[20] H. Yan, G. Buticchi, J. Yang, W. Zhao, H. Zhang, and C. Gerada, "Active thermal control for power converters in modular winding permanent magnet synchronous motor," in *Proc. IEEE 13th Int. Conf. Compat., Power Electron. Power Eng. (CPE-POWERENG)*, Apr. 2019, pp. 1–6.
[21] M. Held, P. Jacob, G. Nicoletti, P. Scacco, and M.-H. Poech, "Fast power cycling test of IGBT modules in traction application," in *Proc. 2nd Int. Conf. Power Electron. Drive Syst.*, vol. 1, May 1997, pp. 425–430.
[22] M. Matsuishi and T. Endo, "Fatigue of metals subjected to varying stress," in *Proc. Jpn. Soc. Mech. Eng.*, Mar. 1968, pp. 37–40.
[23] M. Musallam and C. M. Johnson, "An efficient implementation of the rainflow counting algorithm for life consumption estimation," *IEEE Trans. Rel.*, vol. 61, no. 4, pp. 978–986, Dec. 2012.
[24] L. R. GopiReddy, L. M. Tolbert, B. Ozpineci, and J. O. P. Pinto, "Rainflow algorithm-based lifetime estimation of power semiconductors in utility applications," *IEEE Trans. Ind. Appl.*, vol. 51, no. 4, pp. 3368–3375, Jul. 2015.
[25] V. Raveendran, M. Andresen, G. Buticchi, and M. Liserre, "Thermal stress based power routing of smart transformer with CHB and DAB converters," *IEEE Trans. Power Electron.*, vol. 35, no. 4, pp. 4205–4215, Apr. 2020.
[26] V. N. Ferreira, N. Vazquez, B. Cardoso, and M. Liserre, "Hybrid multiple-active bridge for unequal power flow in smart transformers," in *Proc. IEEE Energy Convers. Congr. Expo. (ECCE)*, Sep. 2019, pp. 5016–5021.
[27] M. Andresen, J. Kuprat, V. Raveendran, J. Falck, and M. Liserre, "Active thermal control for delaying maintenance of power electronics converters," *Chin. J. Electr. Eng.*, vol. 4, no. 3, pp. 13–20, Sep. 2018.
[28] F. Hahn, M. Andresen, G. Buticchi, and M. Liserre, "Thermal analysis and balancing for modular multilevel converters in HVDC applications," *IEEE Trans. Power Electron.*, vol. 33, no. 3, pp. 1985–1996, Mar. 2018.
[29] Y. Ko, M. Andresen, G. Buticchi, and M. Liserre, "Thermally compensated discontinuous modulation strategy for cascaded H-Bridge converters," *IEEE Trans. Power Electron.*, vol. 33, no. 3, pp. 2704–2713, Mar. 2018.

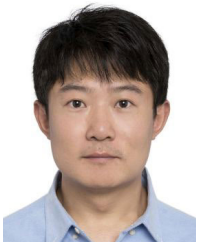

HAO YAN (Member, IEEE) received the B.S., M.S., and Ph.D. degrees in electrical engineering from the Harbin Institute of Technology, Harbin, China, in 2011, 2013, and 2018, respectively.

From 2017 to 2019, he was with the Power Electronics, Machines and Control Group, University of Nottingham Ningbo China, Ningbo, China, and worked on power electronics for electrical drives for two years. From 2019 to 2020, he was a Research Fellow with the Rolls-Royce@NTU Corporate Lab, Nanyang Technological University, Singapore. He is currently an Associate Professor with the School of Civil Aviation, Northwestern Polytechnical University, Xi'an, China. His current research interests include permanent-magnet machine drives and power converters in more electric aircraft.

WEIDUO ZHAO (Member, IEEE) received the Ph.D. degree in electrical engineering from the Harbin Institute of Technology, Harbin, China, in 2015.

He is currently a Senior Research Fellow with the Power Electronics, Machines and Control Group, University of Nottingham Ningbo China, Ningbo, China. His research interests include high-performance electric machines and drives, pulsed power systems, and thermal management. He was a recipient of the Peter J. Kemmey Memorial Scholarship from the 17th International Electromagnetic Launch Symposium, San Diego, CA, USA, in 2014.

GIAMPAOLO BUTICCHI (Senior Member, IEEE) received the master's degree in electronic engineering and the Ph.D. degree in information technologies from the University of Parma, Italy, in 2009 and 2013, respectively.

In 2012, he was a Visiting Researcher with the University of Nottingham, U.K. From 2014 to 2017, he was a Postdoctoral Researcher and the Von Humboldt Postdoctoral Fellow with the University of Kiel, Germany. In 2017, he was appointed as an Associate Professor in Electrical Engineering with the University of Nottingham Ningbo China and as the Head of Power Electronics with the Nottingham Electrification Center. In 2020, he was promoted to a Professor. He is currently one of the advocates for DC distribution systems and multi-port power electronics onboard the future aircraft. He is the author/coauthor of more than 210 scientific articles. His research interests include power electronics for renewable energy systems, smart transformer fed micro-grids, and dc grids for the more electric aircraft.

Dr. Buticchi is an Associate Editor of the IEEE TRANSACTIONS ON INDUSTRIAL ELECTRONICS, the IEEE TRANSACTIONS ON TRANSPORTATION ELECTRIFICATION, and the IEEE OPEN JOURNAL OF THE INDUSTRIAL ELECTRONICS SOCIETY. He is the Chair of the IEEE Industrial Electronics Society Technical Committee on Renewable Energy Systems.

CHRIS GERADA (Senior Member, IEEE) received the Ph.D. degree in numerical modeling of electrical machines from the University of Nottingham, Nottingham, U.K., in 2005.

He subsequently worked as a Researcher with the University of Nottingham on high-performance electrical drives and on the design and modeling of electromagnetic actuators for aerospace applications. He was appointed as a Lecturer in Electrical Machines, in 2008, as an Associate Professor, in 2011, and as a Professor, in 2013, with the University of Nottingham. His main research interest includes the design and modeling of high-performance electric drives and machines. He serves as an Associate Editor for the IEEE TRANSACTIONS ON INDUSTRY APPLICATIONS and the Chair for the IEEE IES Electrical Machines Committee.